Received: 11 October 2023 | Revised: 15 December 2023 | Accepted: 16 January 2024 | Published online: 17 January 2024

RESEARCH ARTICLE

Archives of Advanced Engineering Science
2025, Vol. 3(2) 100–110
DOI: 10.47852/bonviewAAES42021869

BON VIEW PUBLISHING

Battery, Super Capacitor-Based Hybrid Energy Storage with PV for Islanded DC Microgrid

Yam Krishna Poudel[1,*], Ramesh Kumar Pudasaini[1], Anand Kandel[2] and Nava Raj Karki[3]

[1]*Department of Electrical and Electronics Engineering, Nepal Engineering College, Nepal*

[2]*The British College, Nepal*

[3]*Department of Electrical Engineering, IoE TU, Nepal*

Abstract: Cogitating the present national as well as global context, renewable energy sources are becoming increasingly popular as a source of electricity, where connecting to the utility grid is either impossible or excessively costly. Several trends that have emerged as electrical distribution technology in the twenty-first century will change the requirements for energy transmission. Green power generating methods are receiving more attention due to the world's deteriorating environmental conditions, growing prices, the limited nature of fossil fuels, and rising energy demand. The increasing depletion of fossil fuels and the escalating need for energy have made renewable energy sources a global topic of discussion. The incredible advancement of renewable energy has allowed us to address environmental problems. However, the production from these sources could be more predictable, which requires an appropriate energy storage system. The main aim of this research paper is to study the hybrid energy storage with solar photovoltaic for islanded DC microgrid (MG). This research study simulates, analyzes, and presents an islanded mode DC MG with solar photovoltaic (PV), battery, and super capacitor through the use of MATLAB simulink. The maximum power point tracking system uses a two-stage DC converter. The regulated battery energy storage system, coupled through a bidirectional converter, helps to maintain a steady DC bus voltage. The transient and steady-state characteristics of the storage systems are examined. This study demonstrates how quickly hybrid energy storage can adapt to sudden changes in the load.

Keywords: battery energy storage system (BESS), DC microgrid, hybrid energy storage system, maximum power point tracking (MPPT), state of charge (SOC)

1. Introduction

The demand for renewable energies has grown dramatically in recent years due to the dearth of fossil fuels and major environmental problems. As a result, in the current global setting, environmentally friendly distributed generation (DG) and associated technologies are increasingly being highlighted as a study field [1, 2]. The microgrid (MG) that is the focus of today's in-depth research results from the numerous dispersed generations forming in the fast-changing power system. The MG may run on AC or DC power [3]. MG comes in two varieties: ACand DC. Since DC MGs are more sophisticated than AC MGs, they can more efficiently deliver electricity to users [4–6]. The DC MG sustain the DG units' increasing capacity to build a perfect power grid by enabling DG's coordinated and interconnected integration into the electrical power grid [7]. Additionally, DC MGs are mostly applicable in industrial settings with DC loads. Examples of these settings include railway, telecommunication, irrigation, and aviation [5]. Additionally, MG significantly impacts highlighting and focusing on dependable sources of supply and adaptable control options, even on the distribution side [8]. As a result of the depletion of fossil fuels and the need for clean, green energy for sustainable development, renewable energy sources are currently being used to their full potential. The transmission and distribution levels of this clean energy are combined. The primary sources are wind and solar photovoltaic electricity. Single DG is nearly impossible because of the unpredictable and sporadic nature of production, necessitating the utilization of the storage system. The popularity of solar hybrid energy storage systems can be attributed to several key factors. These systems offer a reliable and sustainable solution for meeting energy demands. By combining solar and wind power generation, they can harness the benefits of both renewable energy sources, maximizing energy production and reducing reliance on fossil fuels. The integration of energy storage technology enhances the efficiency and reliability of these systems. Energy storage allows for the capture and storage of excess energy during periods of high generation, which can then be utilized during periods of low generation or high demand. This ensures a consistent and stable power supply,

***Corresponding author:** Yam Krishna Poudel, Department of Electrical and Electronics Engineering, Nepal Engineering College, Nepal. Email: yamkp@nec.edu.np

reducing the intermittency issues associated with renewable energy sources. Furthermore, solar hybrid energy storage systems contribute to grid stability and resilience [9]. The combination of multiple energy sources and storage capabilities enables better management of fluctuations in energy supply and demand, reducing the risk of blackouts and improving overall grid performance. Overall, the technical literature supports the adoption of solar hybrid energy storage systems due to their ability to provide sustainable energy, enhance system efficiency, and contribute to grid stability [10, 11]. A distributed generating and storage system gives users reliable, high-quality power. The MG is therefore created as a new model. Power and energy flow management is accomplished via the storage system [12] IEEE.

2. Literature Review

Due to the depletion of fossil fuels and the idea of clean, green energy for sustainable development, renewable energy sources are now being utilized. This renewable energy is mixed at the levels of transmission and distribution. Electricity from wind and solar photovoltaic sources is the main source. Due to the unpredictable and sporadic nature of production, single-DG is practically impossible, necessitating the use of the storage system. The customers of a dispersed producing and storing system receive dependable, superior power. As a consequence, the MG is produced. Utilizing the storage system, it is possible to manage the power and energy flow [13, 14].

Senapati et al. [15] proposed a model of DC MG that comprises of solar photovoltaic array, battery, SC, and a three-step variable DC load. Tahim et al. [11] proposed a novice method of power flow control for a hybrid AC-DC MG with solar photovoltaic energy. Energy storage was also proposed for integrating pulse load. Poudel and Niraula [16] proposed hybrid MG system for Tagajo campus of Tohoku Gakuin University, Japan, and illustrated that the MG and its control system were operated more efficiently. Battery storage and super capacitor hybrid storage systems offer the best solution for energy storage due to their complementary characteristics. Batteries provide high-energy density and long-duration storage, while super capacitors offer high power density and rapid charge/discharge capabilities, resulting in improved overall system performance and efficiency. Das et al. [8] performed islanding at MVAC grid where issues of synchronization during re-closure did not arise for all DG converters [17].

3. Research Methodology

3.1. DC microgrid model

Figure 1 depicts the suggested model for a DC MG. It comprises solar photovoltaic panels, energy storage batteries, and a super capacitor linked to a DC grid and a load. The MPPT approach is used to track the highest amount of power coming from renewable sources [1]. A power electronics interface known as a bidirectional converter is used to transmit power back and forth between a storage system and a DC grid. The voltage level for the solar photovoltaic is increased using a two-stage converter. Batteries and super capacitors are utilized for energy storage. The battery manages the energy flow, and the super capacitor manages the power flow. Over extended periods, batteries have a high energy density and is used to stabilize the energy flow as needed by the power sources, networks, or loads [18]. Batteries, however, are unable to adapt to sudden changes in load. Due to its high-power density and quick discharge rate, the super capacitor is used in this circumstance as it can respond quickly to large power demands [19–21].

Figure 1
DC microgrid model with AC load

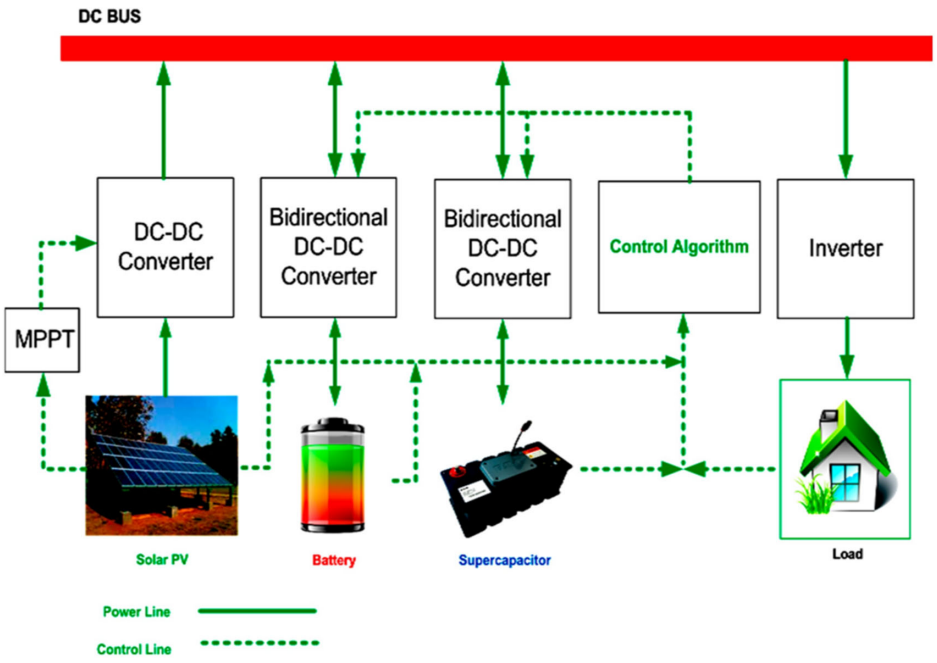

Figure 2
Structure of PV cell

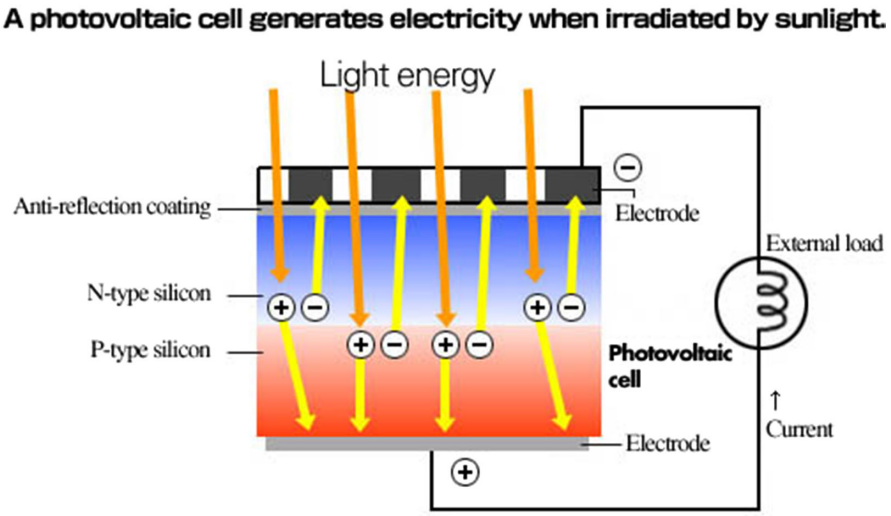

3.2. Solar PV modeling

Here Figure 2 shows the structure of the photovoltaic (PV) cell. It is a semiconductor with boron and phosphorus atoms added to generate a two-layer p-n junction at high temperatures. Positive and negative ions make up these two layers, which correspond to P-holes and N-electrons, respectively. Then, for an electric current flow, a top electrode and a bottom electrode are added. Finally, an antireflective coating is applied to the glass. This cell's main function is to convert light into electrical energy using the photovoltage effect. The resistances are not included in a conventional solar cell, but they are implanted and coupled to the PV diode in a practical application [22].

This is due to factors such as the PV semiconductor's magnitude of resistance and a nonoptimal PN junction diode, which result in the implementation of series and shunt resistance, respectively. Kirchhoff's law can be used to determine the current generator from a solar cell. The equivalent circuit of the PV cell is shown in Figure 3.

$$I_{pv} = I_l - I_d - I_{sh} \tag{1}$$

where I_l is the current generator in

$$I_l = G\{I_{sc}[1 + K_a(T - T_{stc})]\} \tag{2}$$

Figure 3
Equivalent circuit of PV cell

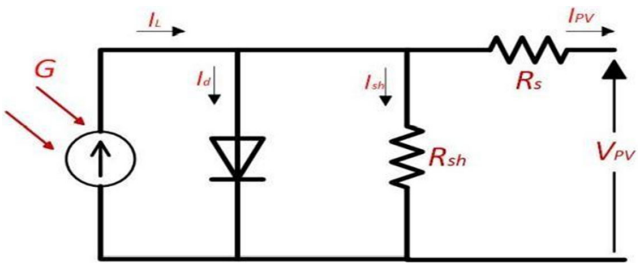

where G is the solar irradiance, T is the climate conditions' ambient temperature, I_{sc} is the PV cell's short circuit current, and K_a is the temperature coefficient. T_{stc} is the PV cell's temperature operation under standard test circumstances (STC), and I_d is the PV diode's current, as determined by Shockley's Equation

$$I_d = I_o\{exp(\frac{qv_d}{nKT}) - 1\} \tag{3}$$

where I_o is the PV diode's saturation current, V_d represents the voltage across the diode, q represents the electrical charge (1.69e–19 C), k represents the Boltzmann constant (1.38e–23 J/K), and n represents the PV diode factor. Now, the universal equation that represents the PV cell's current–voltage (I–V) characteristic chart is

$$I_{pv} = I_l - I_o\left[exp\, exp\left(\frac{q(V_{pv} + I * R_s}{nKT}\right) - 1\right] - \left[\frac{V_{pv} + I * R_s}{R_{sh}}\right] \tag{4}$$

where I_{pv} is the PV output current, and V_{pv} is the PV output voltage.

3.3. Maximum power point tracking

The maximum power point (MPP), the ideal operating point of each photovoltaic cell, changes with cell temperature and irradiance intensity. For PV modules to supply the most easily accessible electricity, this optimization algorithm frequently alters the modules' electrical operating point. One of the simplest and most often used methods is the perturb and observe approach, which works by perturbing current as well as terminal voltage of the array, analyzing and comparing output power of the solar photovoltaic through the aid of preceding perturbation cycle. By adjusting the duty cycle in this case, the MPPT tracks the boost converter [23, 24]. Figure 4 elucidates the flowchart for MPPT.

The P&O algorithm is commonly selected for PV-MPPT methods due to its affordability and user-friendly nature. This approach utilizes the voltage and current measurements obtained from the PV array to determine the power generated by the PV. By comparing these measurements to the previous power level, the

Figure 4
Flowchart for MPPT

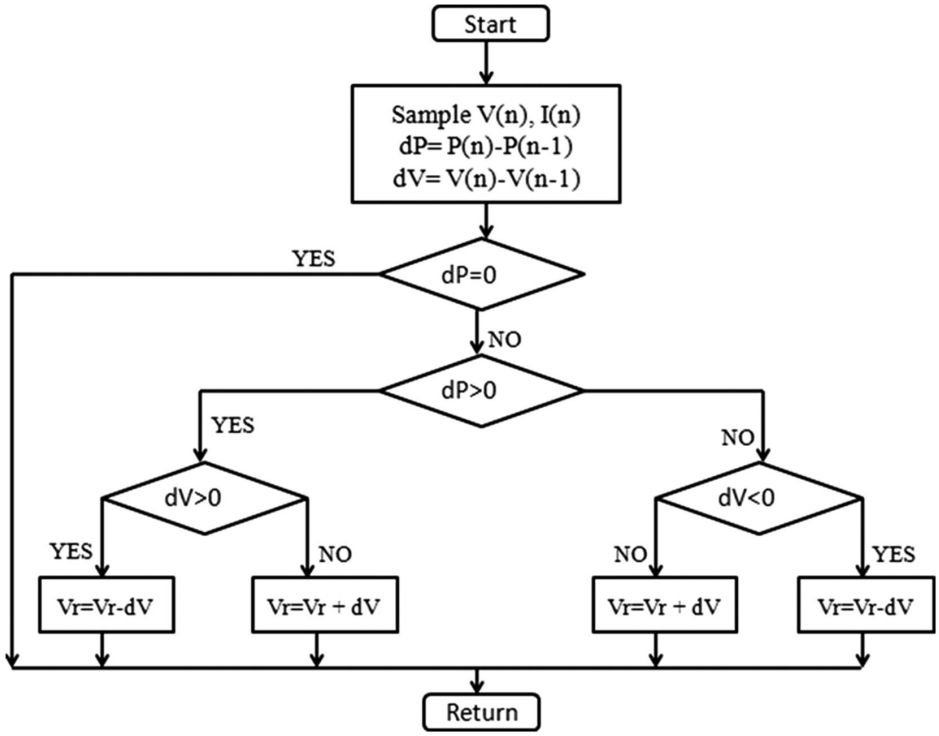

duty cycle of the DC-DC converter is adjusted. This process assists in determining the appropriate direction for the P&O algorithm.

$$D(k+1) = D(k) \pm \Delta D \tag{5}$$

D represents the magnitude of a small increment taken by the variable D, while $D\,(k+1)$ and $D\,(k)$ denote the changes that occurred to D before and after. The P&O algorithm follows a consistent direction when the voltage and power of the PV array increase due to an augmentation in D. Conversely, it moves in the opposite direction when these values decrease. This iterative process persists until the algorithm reaches the optimal point of productivity, at which it oscillates above and below that point. Table 1 provides an overview of the fundamental attributes governing the direction of the P&O algorithm.

Table 1
P&O algorithm with probabilities of direction

ΔP	ΔV	Direction of perturbations
+	+	+
+	−	−
−	+	−
−	−	+

3.4. Boost converter

This step-up converter works on the fundamental two-state ON/OFF concept to increase the input DC voltage to the output. Figures 5 and 6 show the functional circuit and state condition of DC-DC boost converter, respectively.

The output voltage of boost converter is given by

$$V_0 = \frac{1}{1-\alpha} \times V_s \tag{6}$$

where α is the duty cycle. As the cycle increases from 0 to 1, it is clearly seen from the above expression that output voltage always exceeds the input voltage. It also increases with α, theoretically, reaching infinity as α approaches 1 [25]. Consequently, this converter is also known as a step-up converter. The state condition of DC-DC boost converter is shown in Figure 6.

Table 2 depicts the comparisons of different characteristics of batteries and super capacitor. It shows that the battery and super capacitor has complementary character.

Table 2
Comparison of characteristics of batteries and super capacitor

Technology	Lead acid batteries	NaS batteries	Super capacitor
Life cycle (times)	500–1000	+45000	1 millions
Charge time scale	1–5, 5–20 h	30 s to 7 h	0.3 to 30 s
Operating temperature	−20 °C to +65 °C	+300 °C	−40 °C to +75 °C
Pulse load	0.5 to 50 A	20 to 80 A	0.1 to 100 A
Round trip efficiency	63–80%	89–95%	85–98%
Energy density	8 to 600 Wh/kg	170 to 400 Wh/kg	0.05 to 10 Wh/kg
Power density	0.005 to 0.4 Kw/kg	0.01 Kw/kg	0.01 to 10.3 Kw/kg

Figure 5
Functional circuit of boost converter

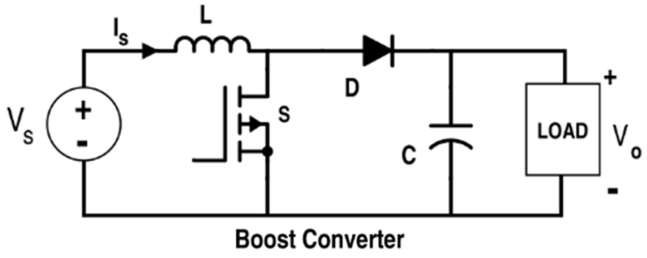

Figure 6
State condition of DC-DC boost converter

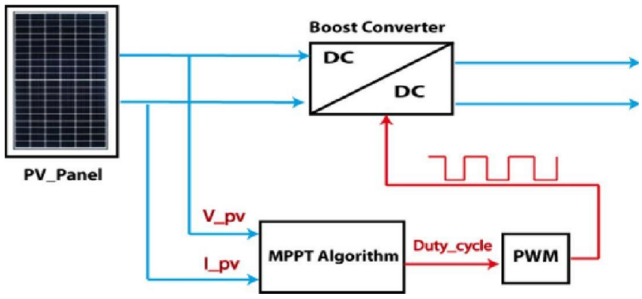

3.5. Super capacitor model

The electrical behavior of an electrostatic capacitor in terms of capacitance and charging current is given by

$$C = \frac{Q}{V} = \frac{\varepsilon S}{d} \tag{7}$$

$$i_c = C\frac{dV}{dt} \tag{8}$$

where C, Q, , V, and i_c are capacitance of the component in Farads, charge in Coulombs, dielectric constant of the dielectric, electric potential in Volts, and current through the capacitor, respectively.

3.6. Battery model

Figure 7 represents the flowchart for modeling of the battery. The equation of the battery model is given by

$$V_{batt} = V_o - R.i - K.\frac{Q}{Q - i.t}(i.t + t*) + Exp(t) \tag{9}$$

$$V_{batt} = V_o - R.i - K.\frac{Q}{i.t - 0.1Q}(i*) - \frac{KQ}{Q - i.t}.it + Exp(t) \tag{10}$$

3.7. Microgrid control

The DC grid controller's primary goal is maintaining the DC MG's voltage while ensuring a balanced power flow between the various energy sources and loads. The "think globally, act locally" concept or philosophy underpins this control system, which is realized using a system of systems methodology [12, 26].

Figure 7
Modeling of battery

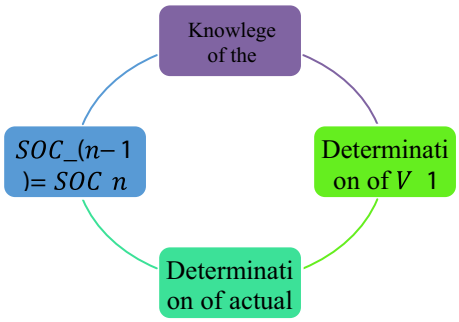

The power flow management for islanded mode DC MG is given by

$$P_{st} + P_{PV} = P_L \tag{11}$$

where $P_{st} = P_{batt} + P_{sc}$, P_{st} is the storage system power, P_{PV} is the solar photovoltaic power, and P_L is the load power. Here P_{batt} *and* P_{sc} are the battery power and super capacitor power, respectively.

3.8. PID controller

The conventional approach to tuning controllers relies on a trial and error method, which proves challenging to apply in different scenarios. This method requires constant adjustment of parameter values and observation of the system's response, resulting in a time-consuming and labor-intensive process. Moreover, there is no assurance that the outcome obtained after numerous iterations will be optimal. Consequently, all the time and effort invested in solving a specific problem may end up being futile. These limitations highlight the need for employing more advanced strategies to attain the best possible results.

Particle swarm optimization (PSO) was developed by James Kennedy and R.C. Eberhart in 1995. It is an evolutionary computation technique that utilizes stochastic processes to explore search spaces. This method draws inspiration from the collective intelligence and movement of swarms. It is considered a population-based strategy as it is rooted in swarm behavior. Similar to how a bird takes the shortest path when searching for food, this algorithm was designed based on such behavior. It involves a large number of particles, each representing a point in a multidimensional space. These particles navigate the search space by adjusting their velocity, influenced by their understanding of the best solution found so far, both individually and collectively as a swarm. Through interactions with the particle that has achieved the best position, they strive to converge toward that location. This concept of social interaction aptly characterizes the behavior of the algorithm.

There are several advantages of using the PSO algorithm over the two aforementioned algorithms. First, PSO requires minimal adjustments in its settings, making it easier to implement. Unlike other algorithms, PSO does not rely on the concept of "survival of the fittest," meaning that the entire population is actively involved in the optimization process. Additionally, PSO is not affected by the scale or magnitude of the problem, unlike genetic algorithms

Figure 8
Flowchart for PSO algorithm

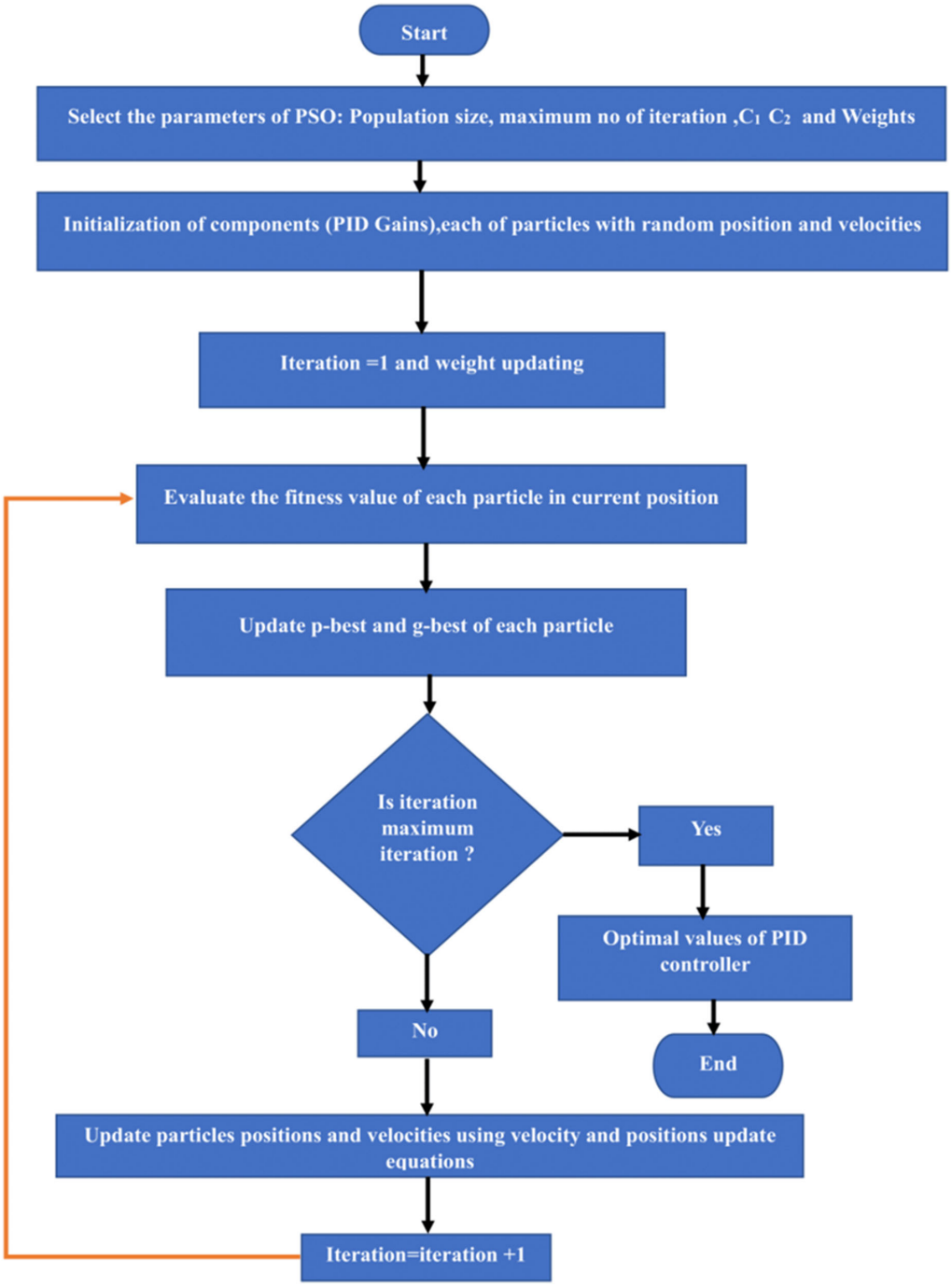

(GA). PSO also overcomes the issue of premature convergence, which is a drawback of GA. Another advantage of PSO is its simplicity, as it only involves two equations, making it straightforward to apply. Even for complex problems, PSO typically requires fewer than a hundred iterations, making it efficient in terms of computational resources. The main equations of PSO algorithm are

Velocity modification equation:

$$V_i^{k+1} = vw_i^k + c_1 rand_1 * (p_{besti} - s_i^K) + c_2 rand_2 * (g_{besti} - s_i^k) \quad (12)$$

where v^k = velocity of agent i at iteration k

Figure 9
(a) Irradiance of solar PV, (b) power obtained from PV and power consumed by load, (c) voltage, current, and power obtained from PV

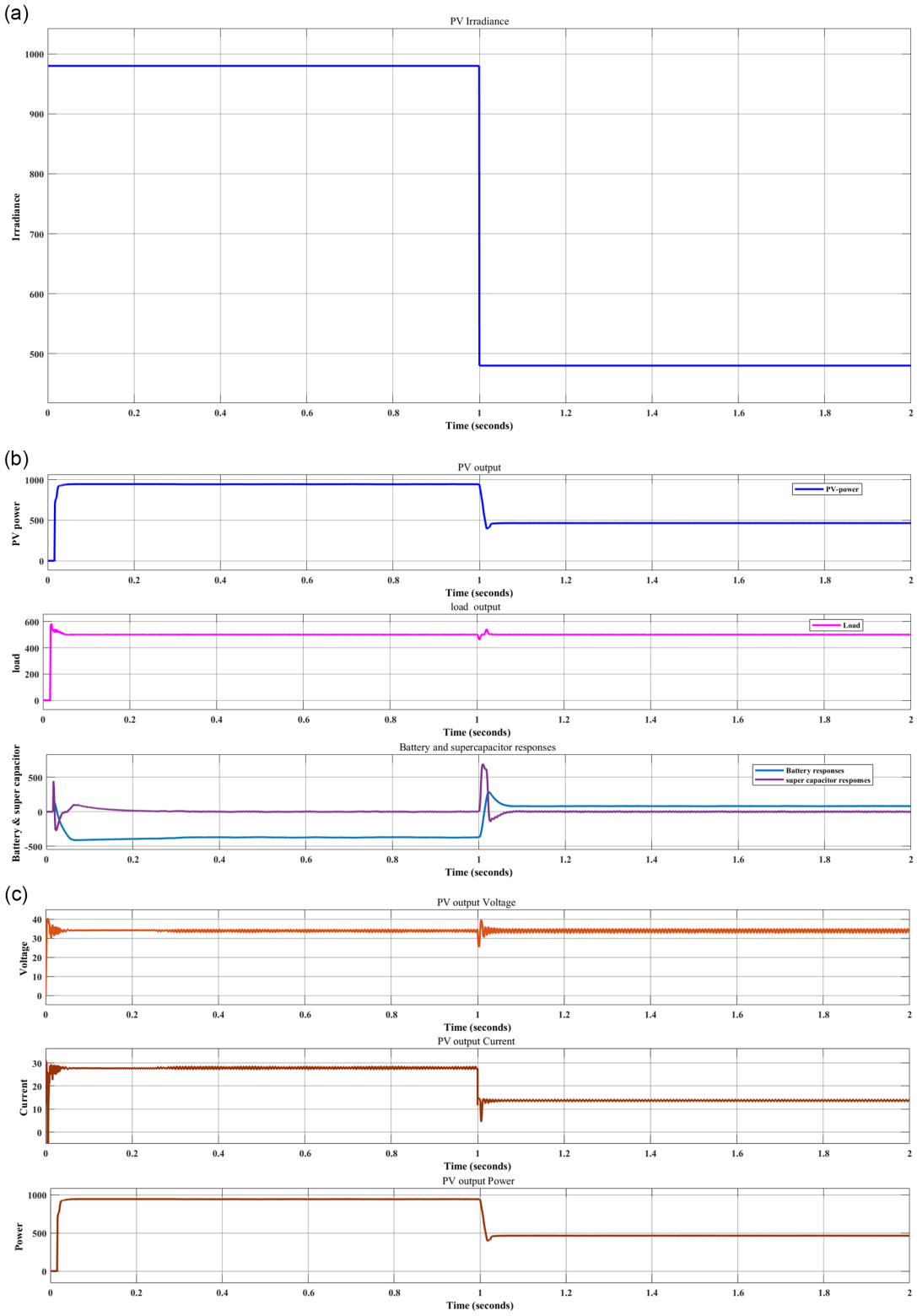

w =weighing function

c_i =weighing factor $rand_i$ =random number between 0 and 1 p_{besti} = p-best of agent i s_i^k=current position of agent i at iteration k g_{besti} = g-best of the group

The first term, wv^k, refers to the component of inertia that causes a particle to move in the same direction it was before. If the value of "w" is low, the convergence will be sped up; otherwise, exploration will be encouraged.

Second term:

$$c_1 rand_1 * (pbest_i - s_i^k) \tag{13}$$

This cognitive component acts as a particle's memory.

Third term:

$$c_2 rand_2 * (gbest_i - s_i^k) \tag{14}$$

The social component that explains why the particle moves to the best region the swarm has discovered thus far. The position of each particle can be updated using the equation of position modification after the velocity of each particle has been computed.

Position modification equation:

$$s_i^{k+1} = s_i^k + v_i^{k+1} \tag{15}$$

where s_i^{k+1} , s_i^k are modified and current search points, respectively.

v_i^{k+1} =Modified velocity

Unless and until specified halting requirements are met, the process is repeated.

3.9. Flow chart for PSO algorithm

Figure 8 illustrates the flow chart for particle swarm algorithm.

4. Result and Discussion

In this study, a hybrid energy storage system comprising both batteries and super capacitors is integrated with a solar photovoltaic system. The system is accurately represented and analyzed using the MATLAB Simulink environment. The simulation duration is defined as 2 seconds, and the corresponding outcomes are presented below.

4.1. Solar PV

The irradiance set for this model is 980 $W/m^2$for one second and 480 W/m^2 is set for the remaining simulation time, which is clearly shown in Figure 9(a). The temperature set for this model is 25° C.

P&O MPPT techniques is used for maximum power point tracking from the solar photovoltaic. The voltage obtained is 35 V, and after one second, it is seen to be decreased. The current decreases from 28 A to 15 A after one second. The total power generated from solar photovoltaic is 960 Watts, which falls to 450 Watts after one second. Figure 9(a), (b), and (c) shows the irradiance level of solar PV, power obtained from the PV and power consumed by load and the voltage, and current and power calculations of PV at different time intervals.

4.2. Battery

The battery voltage decreases to 26 V from 26.5 V after one second. When power is surplus in a system, battery is charged. The negative power indicates the battery charging condition. Albeit, when the generated power is deficit, battery supplies power to the load, and it is in discharging condition. In this case, in the first one second, battery is charging, and in the remaining one second, the battery is discharging. Figure 10 shows the voltage, current, state of charge (SOC), and battery power at different interval of time.

Figure 10
Battery output

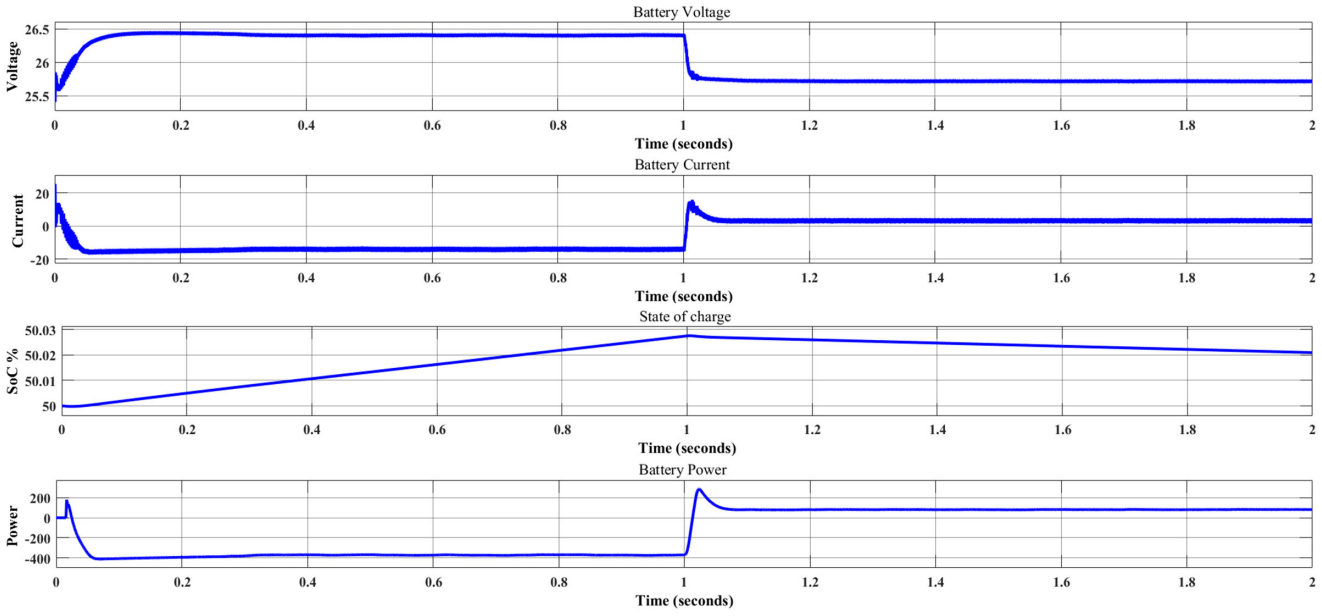

Figure 11
Capacitor voltage–current outputs

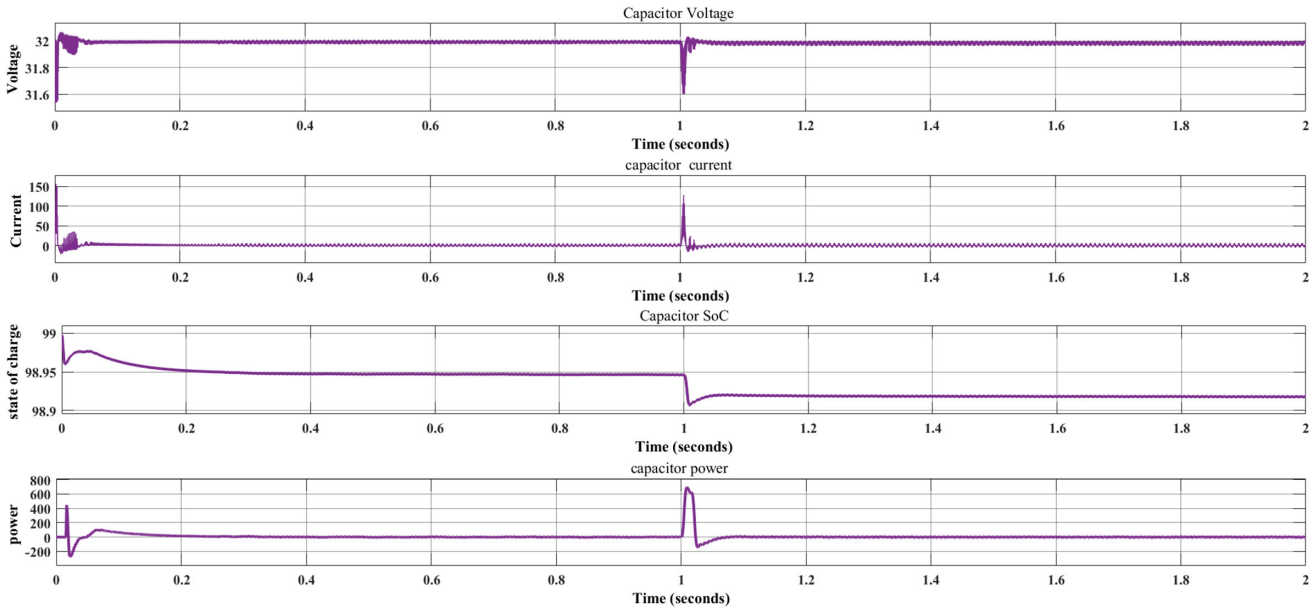

Figure 12
Comparison of output of battery and capacitor performance

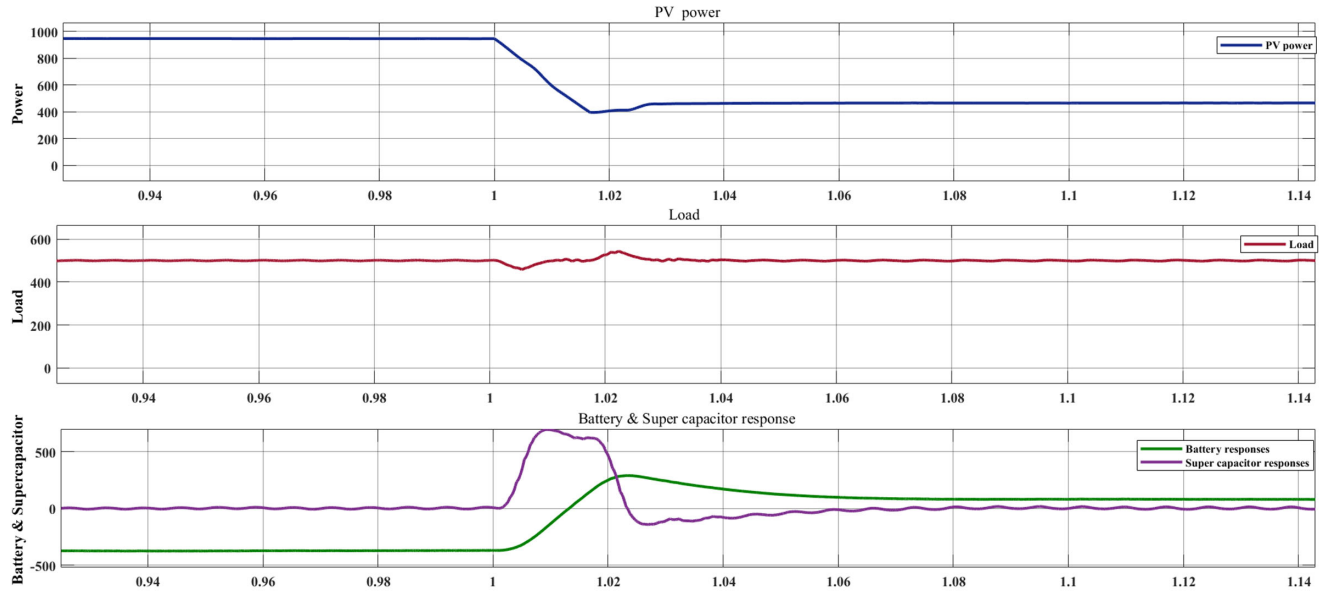

4.3. Capacitor

The voltage diminishes from 32 to 31.6 V after a second for transient condition and finally settles down again to 32 V. The SOC of the capacitor falls down from 98.99 to 98.92%. It supplies the power for a small time. Figure 11 shows the high-power density of the capacitor and it responds in a short time. It clearly depicts that the battery has higher energy density, and super capacitor has the higher power density and is able to respond quickly.

4.4. DC bus voltage

DC bus voltage is maintained at 50 V. When the power and the load fluctuate, its voltage is affected, and this is maintained by the storage system. Figure 12 shows the power generated from PV, total power consumed by the load, and response of the battery and super capacitor at different time intervals. Figure 13 presents the DC bus voltage. Here the super capacitor responds quickly to the load, and battery responds slowly and mitigates the load.

Figure 13
DC bus voltage

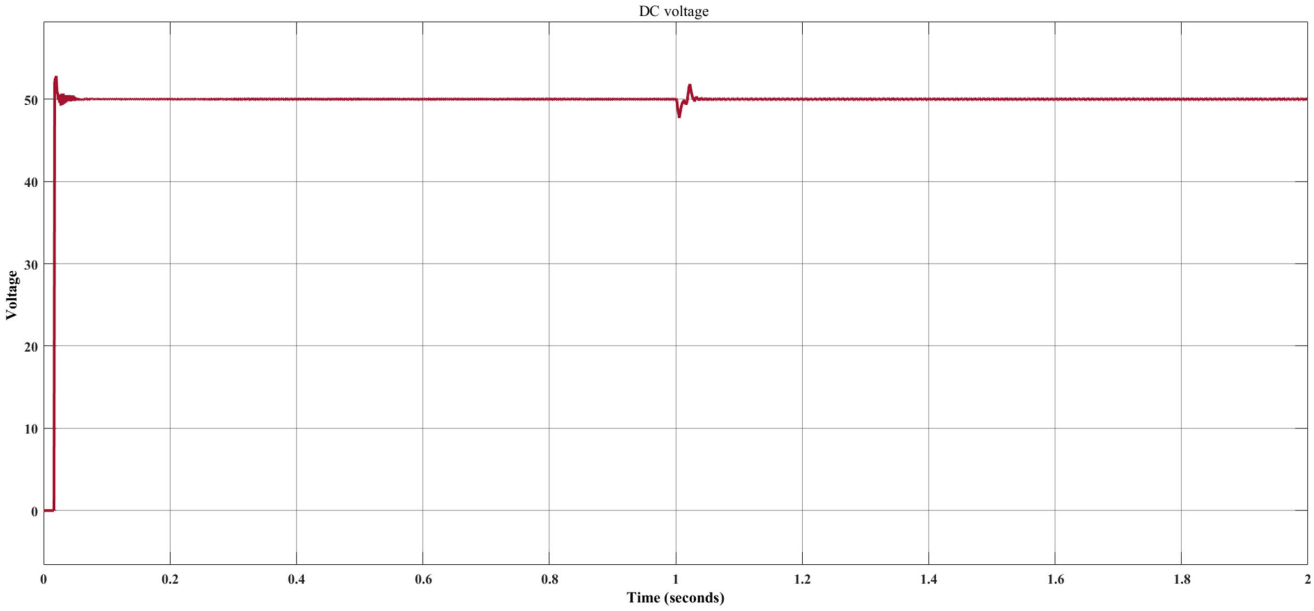

5. Conclusion

From the results obtained, it is seen that the major challenge is to build flexible network integration solutions based on the "Plug and Play" philosophy. Integrating decentralized energy generation, particularly sources like solar photovoltaic technologies, is a crucial yet difficult and complex issue in the near future. An effective strategy to add this power to the main grid and provide ancillary services like voltage, frequency, and inertia support might be to use MG with storage devices.

The integration of intermittent renewable energy sources and their sustainability depend on the storage usage suggested in this paper. The proposed DC MG offers a hybrid storage system that can function on two different time scales. The physical properties of storage components are employed to balance power generation and load demand when power, energy production, and consumption change. From this study, it is seen that control algorithms can keep DC MG stable in the face of sizable and rapid changes in production and demand. The control algorithms are developed that guarantee the stability of DC MG even in the face of extreme production and demand fluctuations. The hybrid energy storage system having a battery with high energy density and the capacitor with high power density is utilized and reflects outstanding performance. The suggested algorithms are found to be simpler and easier to adjust than the current linear control techniques. The suggested approaches can formally guarantee voltage stability and accurately provide a load under reasonable assumptions. Based on the power flow, a hierarchical control strategy employing local converter controllers such as DC-DC converters, an implicit control of main, and secondary is proposed as a remedy.

Ethical Statement

This study does not contain any studies with human or animal subjects performed by any of the authors.

Conflicts of Interest

The authors declare that they have no conflicts of interest to this work.

Data Availability Statement

Data sharing is not applicable to this article as no new data were created or analyzed in this study.

Author Contribution Statement

Yam Krishna Poudel: Conceptualization, Methodology, Software, Validation, Formal analysis, Investigation, Resources, Data curation, Writing – original draft, Writing – review & editing, Visualization, Supervision. **Ramesh Kumar Pudasaini:** Methodology, Validation, Formal analysis. **Anand Kandel:** Software, Formal analysis. **Nava Raj Karki:** Investigation, Resources, Project administration.

References

[1] Musbah, H., Aly, H. H., & Little, T. A. (2021). Energy management of hybrid energy system sources based on machine learning classification algorithms. *Electric Power Systems Research*, *199*, 107436. https://doi.org/10.1016/j.epsr.2021.107436

[2] Yang, X., Li, X., He, H., Zhang, Y., & Xu, Z. (2019). Dynamic power sharing and autonomous voltage regulation in islanded DC microgrids. In *2019 IEEE Power & Energy Society Innovative Smart Grid Technologies Conference*, 1–5.

[3] Wu, G., Kodama, S., Ono, Y., & Monma, Y. (2012). A hybrid microgrid system including renewable power generations and energy storages for supplying both the DC and AC loads. In *2012 International Conference on Renewable Energy Research and Applications*, 1–5.

[4] Kollimalla, S. K., Mishra, M. K., Ukil, A., & Gooi, H. B. (2017). DC grid voltage regulation using new HESS control strategy. *IEEE Transactions on Sustainable Energy*, *8*(2), 772–781.

[5] Liu, Z., Fan, G., Sun, D., Wu, D., Guo, J., Zhang, S., . . . , & Ai, L. (2022). A novel distributed energy system combining hybrid energy storage and a multi-objective optimization method for nearly zero-energy communities and buildings. *Energy*, *239*, 122577. https://doi.org/10.1016/j.energy.2021.122577

[6] Ammari, C., Belatrache, D., Touhami, B., & Makhloufi, S. (2022). Sizing, optimization, control and energy management of hybrid renewable energy system—A review. *Energy and Built Environment*, *3*(4), 399–411. https://doi.org/10.1016/j.enbenv.2021.04.002

[7] Bhattacharjee, S., & Nandi, C. (2021). Design of a voting based smart energy management system of the renewable energy based hybrid energy system for a small community. *Energy*, *214*, 118977. https://doi.org/10.1016/j.energy.2020.118977

[8] Das, D., Hrishikesan, V. M., & Kumar, C. (2020). BESS-PV integrated islanded operation of ST-based meshed hybrid Microgrid. In *2020 IEEE 9th International Power Electronics and Motion Control Conference*, 2122–2128. https://doi.org/10.1109/IPEMC-ECCEAsia48364.2020.9367663

[9] Mahmud, M. A., Roy, T. K., Kumar, R., & Oo, A. M. T. (2020). Nonlinear partial feedback linearizing output feedback control of islanded DC microgrids. In *2020 IEEE International Conference on Power Electronics, Drives and Energy Systems*, 1–5.

[10] Xu, X., Hu, W., Cao, D., Huang, Q., Chen, C., & Chen, Z. (2020). Optimized sizing of a standalone PV-wind-hydropower station with pumped-storage installation hybrid energy system. *Renewable Energy*, *147*, 1418–1431. https://doi.org/10.1016/j.renene.2019.09.099

[11] Tahim, A. P. N., Pagano, D. J., Lenz, E., & Stramosk, V. (2015). Modeling and stability analysis of islanded DC microgrids under droop control. *IEEE Transactions on Power Electronics*, *30*(8), 4597–4607. https://doi.org/10.1109/TPEL.2014.2360171

[12] Poudel, Y. K., Karki, N. R., Gyawali, N. P., & Niraula, D. (2023). Design and control of distributed generations (DGs) for microgrid applications. In *Proceedings of 13th IOE Graduate Conference*, *13*, 256–265.

[13] Eltamaly, A. M., Alotaibi, M. A., Alolah, A. I., & Ahmed, M. A. (2021). A novel demand response strategy for sizing of hybrid energy system with smart grid concepts. *IEEE Access*, *9*, 20277–20294. https://doi.org/10.1109/ACCESS.2021.3052128

[14] Guerrero, J. M., Loh, P. C., Lee, T. L., & Chandorkar, M. (2013). Advanced control architectures for intelligent microgrids – Part II: Power quality, energy storage, and AC/DC microgrids. *IEEE Transactions on Industrial Electronics*, *60*(4), 1263–1270. https://doi.org/10.1109/TIE.2012.2196889

[15] Senapati, B. R., Khilar, P. M., & Sabat, N. K. (2019). An automated toll gate system using vanet. In *IEEE 1st International Conference on Energy, Systems and Information Processing*, 1–5.

[16] Poudel, Y. K., & Niraula, D. (2023). Hybrid energy storage with PV for islanded DC microgrid. *Technical Journal*, *3*(1), 147–158.

[17] Abianeh, A. J., & Ferdowsi, F. (2021). Sliding mode control enabled hybrid energy storage system for islanded DC microgrids with pulsing loads. *Sustainable Cities and Society*, *73*, 103117. https://doi.org/10.1016/j.scs.2021.103117

[18] Keerthana, M. S., Uma, G., & Sowmmiya, U. (2022). A study of a solar PV and wind-based residential DC NanoGrid with dual energy storage system under islanded/ interconnected/ grid-tied modes. *International Journal of Electrical Power & Energy Systems*, *143*, 108473. https://doi.org/10.1016/j.ijepes.2022.108473

[19] Singh, P., & Lather, J. S. (2021). Power management and control of a grid-independent DC microgrid with hybrid energy storage system. *Sustainable Energy Technologies and Assessments*, *43*, 100924. https://doi.org/10.1016/j.seta.2020.100924

[20] Choi, M. E., Lee, J. S., & Seo, S. W. (2014). Real-time optimization for power management systems of a battery/ supercapacitor hybrid energy storage system in electric vehicles. *IEEE Transactions on Vehicular Technology*, *63*(8), 3600–3611. https://doi.org/10.1109/TVT.2014.2305593

[21] Shen, J., & Khaligh, A. (2015). A supervisory energy management control strategy in a battery/ultracapacitor hybrid energy storage system. *IEEE Transactions on Transportation Electrification*, *1*(3), 223–231. https://doi.org/10.1109/TTE.2015.2464690

[22] Ma, T., Serrano, B., & Mohammed, O. (2014). Distributed control of hybrid AC-DC microgrid with solar energy, energy storage and critical load. In *2014 Clemson University Power Systems Conference*, 1–6.

[23] Adhikari, S., & Li, F. (2014). Coordinated V-f and P-Q control of solar photovoltaic generators with MPPT and battery storage in microgrids. *IEEE Transactions on Smart Grid*, *5*(3), 1270–1281. https://doi.org/10.1109/TSG.2014.2301157

[24] Zoka, Y., Sasaki, H., Yorino, N., Kawahara, K. A. K. K., & Liu, C. C. (2004). An interaction problem of distributed generators installed in a MicroGrid. In *2004 IEEE International Conference on Electric Utility Deregulation, Restructuring and Power Technologies*, *2*, 795–799.

[25] Kumar, M., & Tyagi, B. (2020). Design of a model reference adaptive controller (MRAC) for DC-DC boost converter for variations in solar outputs using modified MIT rule in an islanded microgrid. In *2020 IEEE International Conference on Power Electronics, Smart Grid and Renewable Energy*, 1–6.

[26] Juma, M. I., Mwinyiwiwa, B. M. M., Msigwa, C. J., & Mushi, A. T. (2021). Design of a hybrid energy system with energy storage for standalone DC microgrid application. *Energies*, *14*(18), 5994. https://doi.org/10.3390/en14185994

How to Cite: Poudel, Y. K., Pudasaini, R. K., Kandel, A., & Karki, N. R. (2025). Battery, Super Capacitor-Based Hybrid Energy Storage with PV for Islanded DC Microgrid. *Archives of Advanced Engineering Science*, *3*(2), 100–110. https://doi.org/10.47852/bonviewAAES42021869